

# Control of unstable delayed systems with input saturations and measurement constraints: An electrical cart application \*

G. Sanahuja \* P. García \*\* P. Castillo \* P. Albertos \*\*

\* Laboratory Heudiasyc UMR CNRS 6599, Université de Technologie de Compiègne,

B.P. 20529 60205 Compiègne, France.

e-mail: {gsanahuj, castillo}@hds.utc.fr

\*\* Department of Systems Engineering and Control

Universidad Politécnica de Valencia

P.O. Box. 22012, E-46071, Valencia, Spain.

e-mail: {pggil, pedro}@isa.upv.es

---

**Abstract:** This paper deals with the position control of a mobile vehicle. The main constraints refer to the lack of measurements, presence of input/output delays and actuator saturations. Position measurement of this vehicle is given by a vision system, whose frequency is limited due to picture computation, whereas the control action can be applied at a faster rate. Not only the measurement rate is low, also a conversion delay must be considered. Additional delays can also appear in the control action updating, where actuator saturations should be considered. This paper demonstrates that the use of a prediction-observer scheme, based on a linear model of the system and executed at a high rate, can stabilize the system. This is done even if the control law is non linear, due to the appearance of saturations, also coping with the input/output delays.

## 1. INTRODUCTION

In mobile robots and automated vehicles, vision sensors are more and more essential in order to resolve complex problems of the environment perception. Its miniaturization and recent image processing developments have allowed the mounting of the visual sensor on the robot/vehicle and the integration of visual information in the control loop.

These developments have permitted the realization of many more robotic tasks such as target tracking and obstacle avoidance. The first works concerning the use of visual information in robot control were presented by ??). They present two separate approaches. The first approach, commonly called ‘look and move’, is synthesized in terms of regulation of the end effector situation. In the second approach, the end effector of a robot is controlled by using visual information. This control scheme is called ‘visual servoing’.

Data acquisition using slow measuring procedures, such as image processing, has more time constraints than actuators and, as a result, different rates could be used for control updating and output sampling. Thus, instead of using the same lowest sampling rate for all the variables in the process, the multirate (MR) approach tries to reach the fastest sampling rate control performances but using the available data, that is, data sampled at different rates ?).

Also, image processing introduces a delay between the image capturing time and the time the information is available for monitoring and/or control purposes. In many practical applications, time delays may be intrinsic to the process to be controlled, such as in chemical and biological processes, distillation columns, processes with thermal exchanges, and so on. Delays can also be introduced in the implementation of the controller itself (computation time of the control algorithm, distributed systems, remote control) or they can appear due to the sharing of communication networks. As previously mentioned, the internal information processing in sensors and/or actuators may also result in additional delays.

In general, the control system performance is very sensitive to delays, even more than to other parameters in the model. In fact, a closed-loop control system may become easily unstable as a consequence of delays. Systems with delay are infinite-dimensional systems, and thus their transfer function has an infinite number of poles. Thus, the tuning of the parameters of a conventional regulator to adjust these poles can be very difficult.

The use of state or output predictors, as for example the very popular Smith Predictor ?, and finite spectrum assignment (FSA), ?, may be considered as the main control methods for linear processes having a significant delay in their input or output, see ?). The initial results were reported for continuous time systems, later on being also applied to regularly sampled-data systems. However a common drawback, linked to the internal instability of the prediction, is that they fail to stabilize unstable systems.

---

\* This work was supported in part by the Ministerio de Educación y Ciencia Español. Mobility Program Ref. PR2006-0489

The issue of missing data is usually tackled by designing a predictor based on the process model to either infer the lacking measurements or estimate the state and all the required process variables, by using a Kalman filter. In ?? a control-prediction scheme to solve the scarce measurements prediction problem with delay is proposed. The use of both approaches, ?? and ??, has shown good performances, but in the first approach the control algorithm is restricted within the MR framework, so if a different control law is required, as for example a non-linear control, the use of this approach is not possible. The use of the second approach is also a good solution, because there is no restriction about the control scheme the system being either stable or unstable, but the use of these techniques requires a relatively high computational cost.

Recently a new method to control unstable systems with time-varying delays has been presented by ??). The proposed algorithm is based on a discrete-time state feedback controller using the prediction of the state. A convergence analysis shows that the state converges to the origin in spite of uncertainties in the knowledge of the plant parameters, the system delay and even variations of the sampling period. The proposed control scheme also has been successfully implemented to control the yaw displacement of a real four-rotor mini-helicopter, see ??). The experimental validation has been developed on an embedded system, MaRTE OS (see ??), which allows the implementation of minimum real-time systems according to standard POSIX.13 of the IEEE.

Other than the consideration of the input/output delays, in this paper we propose a control system for the position of a mobile vehicle dealing with the nonlinearities introduced by the saturation in the actuators and the low rate in getting the vehicle position which is estimated by a laser vision system. The process is open loop unstable and almost impossible to control at the measurement sampling rate imposed by the vision captor. If a prediction-observer scheme based on a linear model is applied to the same system and if a better frequency is used for the control, thus the vehicle behavior can be stabilized. Moreover, the system should remain stable even with additional delays in actuation and/or measurement.

The rest of the paper is organized as follows: first, the ingredients of the problem setting are summarized in the next section. Then, the proposed control solution is derived. This solution is first implemented on a simulated system and later on is applied to a real electric car. The obtained results are discussed and some conclusions are drafted.

## 2. PROBLEM FORMULATION

As previously mentioned, this work is application oriented, the final goal being to control an unstable mobile vehicle under constraints in the actuation and measurement and delays in the sensing device. Thus, time delay counteraction, multirate pattern and saturating control are the ingredients of the proposed solution. Some previous results are summarized in this section.

### 2.1 Prediction-observer based control

A brief revision of the predictor-observed control scheme proposed in ??), for time delayed linear systems, is outlined. For a deeper analysis the reader is remitted to these references, where a more general treatment of this problem is presented.

Let us consider the following continuous-time state space representation of a system with input delay

$$\dot{x}(t) = A_c x(t) + B_c u(t - \tau) \quad (1)$$

where the nominal plant parameter matrices are  $A_c \in \mathbb{R}^{n \times n}$ ,  $B_c \in \mathbb{R}^{n \times m}$  and  $\tau > 0$  is the time delay.

As a computer implementation is intended, let us define the sampling period as  $T = t_{k+1} - t_k$ . Furthermore, it is assumed to simplify the notation that  $\tau = dT$  where  $d \in \mathbb{Z}^+$ .

The discrete-time version of (1), is given by

$$x_{k+1} = Ax_k + Bu_{k-d} \quad (2)$$

where:  $A = e^{A_c T}$ , and  $B = \int_0^T e^{A_c \lambda} d\lambda B_c$ .

Let us assume that

$$\tau = dT = (h + \Delta h)T \quad (3)$$

where  $dT$  is the actual unknown delay,  $hT$  is the delay to be considered for computing the prediction scheme and  $\Delta hT$  is the delay error, where  $\Delta h \in \mathbb{Z}$ , and  $h \in \mathbb{Z}^+$ .

Consider the following control input

$$u_k = -K\hat{x}_{k+h} \quad (4)$$

where  $K \in \mathbb{R}^{m \times n}$ , and define

$$\hat{x}_{k+h} = A^h x_k + A^{h-1} B u_{k-h} + \dots + B u_{k-1} \quad (5)$$

It has been demonstrated in ??) that the prediction  $\hat{x}_{k+h}$  in (5) can be expressed as

$$\hat{x}_{k+h} = x_{k+d} + A^h x_k - A^h x_{k+(d-h)} \quad (6)$$

Concerning the stability of the closed-loop system, the closed-loop system composed of (2), (4), and (5) leads to

$$x_{k+1} = (A - BK)x_k - BKA^h x_{k-d} + BKA^h x_{k-h} \quad (7)$$

Introducing (6) in (4),

$$u_k = -K(x_{k+d} + A^h x_k - A^h x_{k+d-h}) \quad (8)$$

or

$$u_{k-d} = -K(x_k + A^h x_{k-d} - A^h x_{k-h}) \quad (9)$$

Introducing (9) in (2), it yields

$$x_{k+1} = Ax_k - BKx_k - BKA^h x_{k-d} + BKA^h x_{k-h}$$

Defining  $M = (A - BK)$ , and  $A_1 = BKA^h$ , from (7) it yields

$$x_{k+1} = Mx_k + A_1 x_{k-h} - A_1 x_{k-d} \quad (10)$$

Then it has been demonstrated ??) that the system in (10) will be asymptotically stable if there exist positive definite

matrices  $P$ ,  $Q_1$ ,  $Q_2$ ,  $Z_1$  and  $Z_2$ , and matrices  $X_1$ ,  $X_2$ ,  $Y_1$  and  $Y_2$ , such that the following LMI constraints hold.

$$\begin{pmatrix} (1,1) & -Y_1 & -Y_2 & M^T P & h\Gamma^T Z_1 & d\Gamma^T Z_2 \\ -Y_1^T & -Q_1 & 0 & A_1^T P & hA_1^T Z_1 & dA_1^T Z_2 \\ -Y_2^T & 0 & -Q_2 & -A_1^T P & -hA_1^T Z_1 & -dA_1^T Z_2 \\ PM & PA_1 & -PA_1 & -P & 0 & 0 \\ hZ_1^T \Gamma & hZ_1^T A_1 & -hZ_1^T A_1 & 0 & -hZ_1 & 0 \\ dZ_2^T \Gamma & dZ_2^T A_1 & -dZ_2^T A_1 & 0 & 0 & -dZ_2 \end{pmatrix} < 0 \quad (11)$$

$$\begin{pmatrix} X_1 & Y_1 \\ Y_1^T & Z_1 \end{pmatrix} \geq 0 \quad \begin{pmatrix} X_2 & Y_2 \\ Y_2^T & Z_2 \end{pmatrix} \geq 0 \quad (12)$$

where  $\Gamma := (M - I)$  and

$$(1,1) := -P + hX_1 + dX_2 + Y_1 + Y_1^T + Y_2 + Y_2^T + Q_1 + Q_2$$

**Remark** Note that if  $d = h$ , then  $\hat{x}_k = x_k$  (see (6)), therefore (7) yields

$$x_{k+1} = (A - BK)x_k$$

In general the state of the system is not fully accessible and therefore we require an observer to estimate the state. In ?) the stability of the system when the state is estimated using a state observer is also proved, as the separation principle between the observer and the predictor is fulfilled.

## 2.2 Multirate sensor

Now, let us consider the output availability. Assume that the output equation is:

$$y_k = Cx_k \quad (13)$$

but the measurement is only accessible once every  $N$  time instants,  $NT$  being the image processing rate.

To implement (4), the state should be available at any sampling period. The observer or virtual sensor is designed following the ideas in ?), based on the plant model (2):

$$\hat{x}_{k+1} = A\hat{x}_k + Bu_{k-d} + Lm_k(y_k - \hat{y}_k), \quad (14)$$

$$\hat{y}_k = C\hat{x}_k. \quad (15)$$

where  $L$  is the observer matrix and  $m_k = 1$  if the measurement is available and  $m_k = 0$  if it is not. That is, the estimation updating is only activated when a new measurement is accessible.

The innovation term,  $Lm_k(y_k - \hat{y}_k)$ , should be designed to assure the state estimation error convergence:

$$\tilde{x}_k = x_k - \hat{x}_k; \quad \lim_{k \rightarrow \infty} \tilde{x}_k = 0 \quad (16)$$

Considering the state estimation evolution over  $N$  sampling periods, it yields

$$\tilde{x}_{k+N} = \mathcal{A}\tilde{x}_k = (I - LCA^{-d}) A^N \tilde{x}_k \quad (17)$$

The necessary and sufficient condition to stabilize the predictor is to take a matrix  $L$  such that all eigenvalues of  $\mathcal{A}$  are inside the unit circle. See (?) where a detailed treatment of virtual sensors design can be found.

## 2.3 Actuator saturation

To complete the problem setting, the actuators saturation must be considered. That means, the linear control law, as presented in (4), cannot be applied if the absolute value of the control action is out of limits.

Thus, the control law should be such as

$$u_k = -\sigma[K(\hat{x}_{k+h})] \quad (18)$$

where  $\sigma(s)$  is a ramp-shaped saturation function such that  $\forall s, |\sigma[s]| \leq U_{max}$ .

An analysis of the closed-loop stability for simple rate, undelayed plants is reported in ?).

## 3. EXPERIMENTAL PLATFORM

### 3.1 Presentation of the platform



Fig. 1. Experimental cart

The experimental platform (see Figure 1) is composed by an electrical cart moving only along the  $x$  axis, a vision-laser sensor and the Matlab XPC target system. The distance  $d$  between the cart and the wall is measured using a new low-cost sensor composed by a camera and a laser. The camera is ‘looking’ a point in the wall produced by a laser pointer, then the image is sent to a ground computer station (PC vision) to estimate and express the distance with respect to a ground frame coordinates system. In this paper we assume the calibration of the system  $\{camera, laser\}$  is done.

The resulting  $x$ -position is sent to the ground station computer to compute the control inputs using XPC Target and the RS232 serial communication. The control input is sent to the cart’s motors through Advantech PCL-726 output card. Due to physical constraints in the cart’s motors, the control input signal should satisfy the following inequality:

$$0V < \tau_1 < 5V$$

### 3.2 Dynamic model of the vehicle

We will apply the proposed control scheme to stabilize the electrical cart in the  $x$ -coordinate. The dynamical equation of the cart in the  $x$ -axis (see Figure 2) could be obtained scheming it in 2D, with two identical wheels and a chassis (see Figures 3–5). We will denote  $m$  the mass of each wheel,  $C_i$  its center (which is assumed to be also its center of gravity),  $r$  its radius and  $J$  its moment of inertia. For the chassis we will denote  $M$  its mass and  $L$  the distance between wheels. The center of gravity of the chassis is

assumed to be on its middle. The contact between ground and wheels is assumed to be a point, and the study will be done in the case of limiting friction for each wheel.

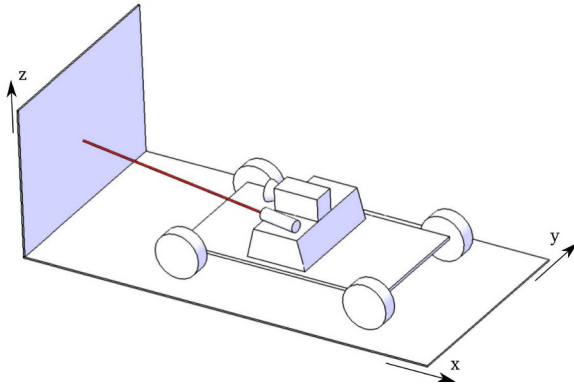


Fig. 2. Scheme of the cart

Each wheel  $i$ ,  $\forall i = 1, 2$ , is subjected to the following forces: a) its weight  $P_i = mg$ , b) the reaction force,  $R_i$ , from the ground and c) the force,  $F_{ch/i}$ , from the chassis applied in the axis of the wheel. Under the hypothesis of limiting friction, we have :  $\vec{R}_i = F_{f,i} \cdot \vec{x} + N_i \cdot \vec{z}$  and  $F_{f,i} = \mu N_i$ , with  $\mu$  the coefficient of friction between wheel and ground. The torque applied to the axis of the wheel is denoted by  $\tau_i$ . For the driving wheel, i.e. the driving torque and for the free wheel the torque is due to the friction in the axis. Moreover, the chassis is subjected to its weight  $P = Mg$ , applied in its center.

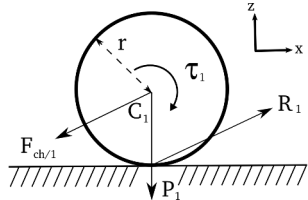


Fig. 3. Driving wheel

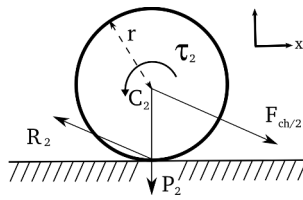


Fig. 4. Free wheel

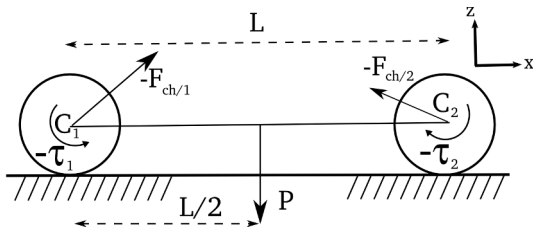


Fig. 5. Chassis of the cart

From Figures 3–5 and using Newton's equations, we obtain the following equations for the driving wheel

$$\mu N_1 - \overrightarrow{F_{ch/1}} \cdot \vec{x} = m\ddot{x} \quad (19)$$

$$-mg - \overrightarrow{F_{ch/1}} \cdot \vec{z} + N_1 = 0 \quad (20)$$

$$\tau_1 - r\mu N_1 = \frac{J}{r}\ddot{x} \quad (21)$$

The dynamic for the free wheel is described by,

$$-\mu N_2 + \overrightarrow{F_{ch/2}} \cdot \vec{x} = m\ddot{x} \quad (22)$$

$$-mg - \overrightarrow{F_{ch/2}} \cdot \vec{z} + N_2 = 0 \quad (23)$$

$$-\tau_2 + r\mu N_2 = \frac{J}{r}\ddot{x} \quad (24)$$

and for the chassis is

$$\overrightarrow{F_{ch/1}} \cdot \vec{x} - \overrightarrow{F_{ch/2}} \cdot \vec{x} = M\ddot{x} \quad (25)$$

$$-Mg + \overrightarrow{F_{ch/1}} \cdot \vec{z} + \overrightarrow{F_{ch/2}} \cdot \vec{z} = 0 \quad (26)$$

$$-\tau_1 + \tau_2 - L\overrightarrow{F_{ch/2}} \cdot \vec{z} + Mg\frac{L}{2} = 0 \quad (27)$$

After some algebraic manipulations using (19)–(27), we obtain,

$$\ddot{x} = k_\tau \tau_1 + k_\mu \quad (28)$$

with

$$k_\tau = \frac{Lr}{\mu r^3(2m + M) + J(2\mu r + L)} \quad (29)$$

$$k_\mu = \frac{-\mu g L r^2 (m + M/2)}{\mu r^3(2m + M) + J(2\mu r + L)} \quad (30)$$

Note that (28) is the classical mathematic equation of a cart moving in the  $x$ -axis. The last term,  $k_\mu$ , in this equation could be considered as the friction.

### 3.3 Non linear control law

To stabilize the cart in a  $x_d$  desired position we will use a non linear control law based on saturation functions.

Let us propose the following non linear control law to stabilize the cart in the  $x$ -coordinate

$$\tau_1 = -[\sigma_d(k_d \dot{x}) + \sigma_p(k_p(x - x_d)) + k_\mu]/k_\tau \quad (31)$$

where  $k_p$  and  $k_d$  are positive constant and  $\sigma(s)$  is a ramp-shaped saturation function such that  $\forall s, |\sigma_b(s)| \leq b, b \in \mathbb{R}$ .

Introducing (31) into (28) we obtain

$$\ddot{x} = -\sigma_d(k_d \dot{x}) - \sigma_p(k_p(x - x_d)) \quad (32)$$

As already mentioned, the stability analysis of this closed-loop system was proved in ?).

## 4. SIMULATIONS

The continuous time model of the cart is (28). Based on the parameters from the experimental platform, the linear model is:

$$\dot{\bar{x}} = A\bar{x} + Bu \quad (33)$$

where  $\bar{x} = [x_1 = x, x_2 = \dot{x}]^T$ ,  $A = \begin{bmatrix} 0 & 1 \\ 0 & 0 \end{bmatrix}$ ,  $B = \begin{bmatrix} 0 \\ k_\tau \end{bmatrix}$  and  $u = \tau_1$ . For our study, the term  $k_\mu$  is considered as perturbations in the system.

The image capturing and processing introduces a delay of  $L_r = 1s$ . Moreover, it is not possible to sample the image faster than 500 ms. Thus, the output sampling period is  $NT = 0.5s$ . As already mentioned, the input is bounded ( $0 \leq u \leq 5V$ ).

If the plant model is discretized at this period ( $NT$ ), the control action required to stabilize the cart immediately saturates. If the input updating period is reduced to  $T = 0.01\text{s}$ , a multirate scheme can be used.

The observer gain to fulfil (16) is chosen as  $L = [268.80 \ 3.28]'$ . Gains used for the control law are :  $k_p = 0.1$ ,  $k_d = 0.5$ . Bounds for saturation are  $p = \pm 0.5$  (the proportional part) and  $d = \pm 1.5$  (the derivative part).

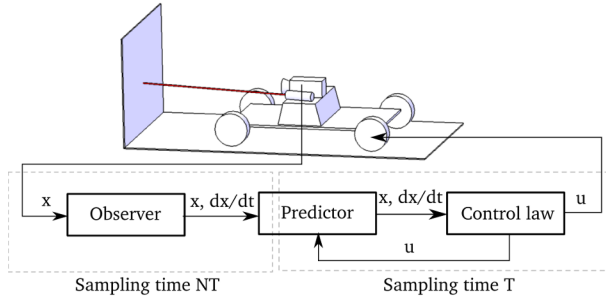


Fig. 6. Control system scheme.

Thus, we propose two situations:

- 1 Dealing with a multi-rate situation, with a sample rate of  $NT = 0.5\text{s}$  and an actuator working at the sample rate of  $T = 0.01\text{s}$ , the step responses with and without the proposed predictor are shown in figure 7. The instability of the system without predictor is clearly shown.

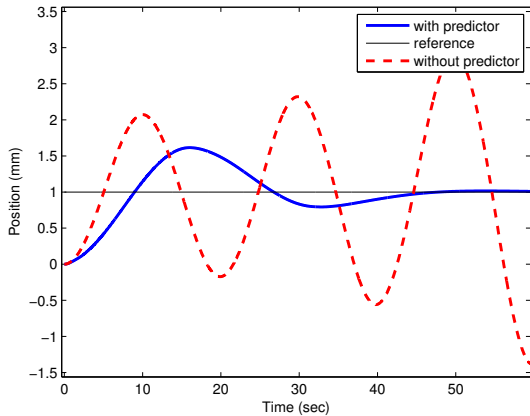


Fig. 7. Multi-rate, without delay

- 2 The same scheme as above (sample rate of  $NT = 0.5\text{s}$ , actuator sample rate  $T = 0.01\text{s}$ ) plus an actuator delay of  $L_r = 1\text{s}$  gives the results showed in figure 8. The simulation is done with and without the proposed predictor. It also shows the instability of the system without predictor.

## 5. EXPERIMENTAL RESULTS

In this section, the parameters used are the following:

- observator gain :  $L = [0.02 \ 0.12]'$ ,
- control law gains :  $k_p = 0.05$ ,  $k_d = 0.001$ ,

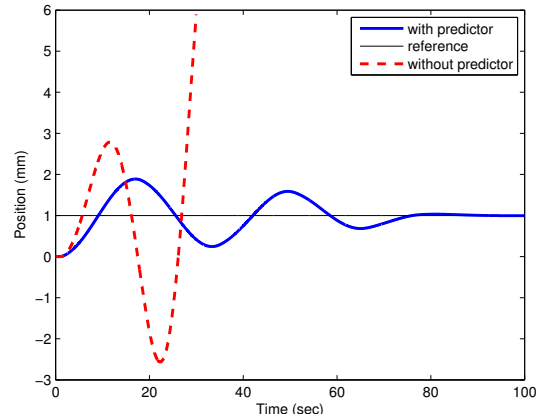


Fig. 8. Multi-rate, with actuator delay

- bounds for saturator :  $p = \pm 0.5$  (proportional part),  $d = \pm 1.5$  (derivative part).

In the experimental setting, we tried to reproduce the same cases as in simulations. Thus we made four experiments:

- 1 A multi-rate scheme, with a sample rate of  $NT = 0.5\text{s}$  and an actuator working at the sample rate of  $T = 0.01\text{s}$ .
- 2 Same scheme as above, using the proposed predictor.
- 3 Same scheme as the first one, adding a delay in actuator of  $L_r = 1\text{s}$ .
- 4 Same scheme as above, using the proposed predictor.

Results are respectively shown on figures 9, 10, 11 and 12.

Figure 9 shows that the system cannot reach the desired position in such conditions. Indeed, the measurement sample rate is too slow. But the addition of the proposed predictor helps the stabilization, as shown in figure 10.

As shown in figure 11, the addition of the actuator delay makes the system unstable, if no predictor is used. The same experiment with the predictor, showed in figure 12, gives better results. In this experiment, we see that the system sometimes oscillates a little (but less than without predictor) and sometimes is stable. This might be due to the high delay in actuator (100 times the sample rate), and to the uncertainty of the car's model.

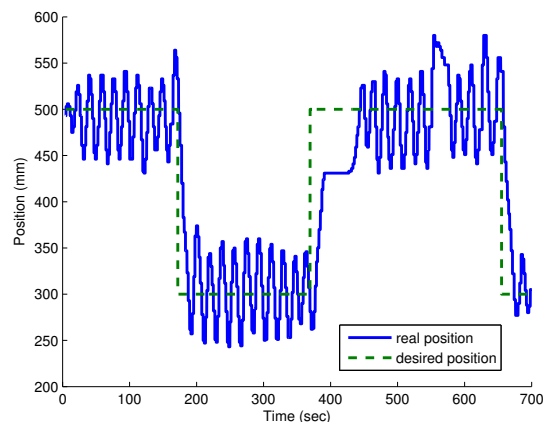


Fig. 9. Experiment without predictor, without delay

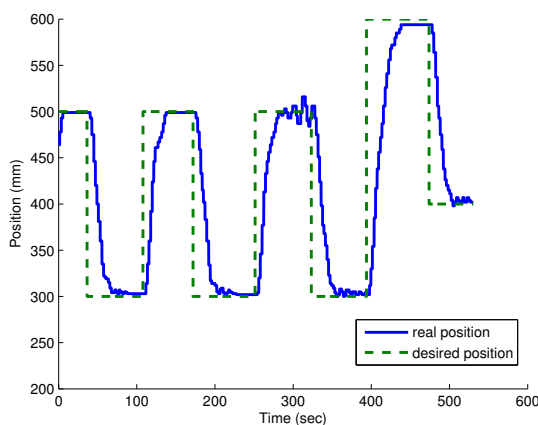


Fig. 10. Experiment with predictor, without delay

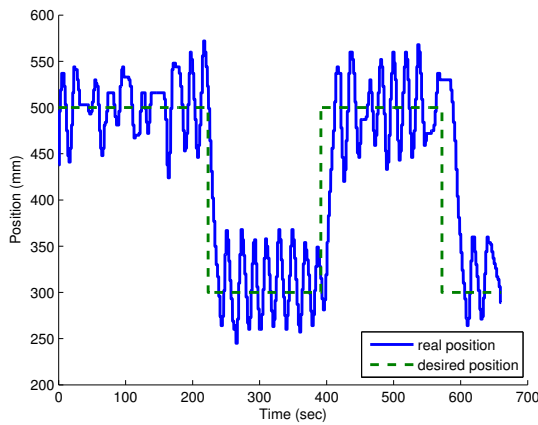


Fig. 11. Experiment with delay but without predictor

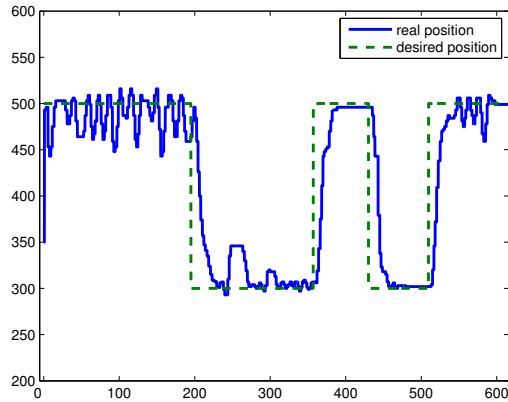


Fig. 12. Experiment with delay and predictor. Note that in this case, the real initial position is 350 mm.

## 6. CONCLUSION

In this paper we propose a non linear law coping with saturations to control the position of a mobile vehicle, estimated by a laser vision system. Due to the computational time of each image, the system is unstable using the frequency given by the vision sensor. Yet, if a prediction-

observer scheme based on a linear model is applied to the same system and if a faster frequency is used for the control then the resulting system becomes stable. Moreover, the system remains stable even with additional delays in actuator and/or measurement.

Unlike others papers of control for multi rate systems, the proposed scheme is independent of the control law used. Moreover, the scheme is quite simple and robust against model or sample rate errors and also against noise in data.

## 7. ACKNOWLEDGMENTS

This project has been partially granted by the CICYT project number DPI2005-09327-C02-01/02.